

Bi-CoG: Bi-Consistency-Guided Self-Training for Vision-Language Models

Rui Zhu¹ Song-Lin Lv^{1,2} Zi-Kang Wang^{1,2} Lan-Zhe Guo^{1,2} *

¹School of Intelligence Science and Technology, Nanjing University, China

²National Key Laboratory for Novel Software Technology, Nanjing University, China
zhurui@smail.nju.edu.cn, {lvsl,wangzk,guolz}@lamda.nju.edu.cn

Abstract

Exploiting unlabeled data through semi-supervised learning (SSL) or leveraging pre-trained models via fine-tuning are two prevailing paradigms for addressing label-scarce scenarios. Recently, growing attention has been given to combining fine-tuning of pre-trained vision-language models (VLMs) with SSL, forming the emerging paradigm of semi-supervised fine-tuning. However, existing methods often suffer from model bias and hyperparameter sensitivity, due to reliance on prediction consistency or pre-defined confidence thresholds. To address these limitations, we propose a simple yet effective plug-and-play methodology named **Bi-Consistency-Guided Self-Training (Bi-CoG)**, which assigns high-quality and low-bias pseudo-labels, by simultaneously exploiting inter-model and intra-model consistency, along with an error-aware dynamic pseudo-label assignment strategy. Both theoretical analysis and extensive experiments over 14 datasets demonstrate the effectiveness of Bi-CoG, which consistently and significantly improves the performance of existing methods.

Introduction

Addressing downstream tasks with limited labeled data remains a critical challenge in real-world applications (Yang et al. 2022). Two prominent paradigms have emerged to tackle this issue: (1) adapting pre-trained models, such as vision-language models (VLMs) (Radford et al. 2021; Jia et al. 2021), for image classification tasks; and (2) applying semi-supervised learning (SSL) methods that leverage large amounts of inexpensive unlabeled data. Recent work (Lv et al. 2025b) has further suggested combining these two approaches, where the strong zero-shot capabilities of pre-trained VLMs are used to generate reliable pseudo-labels that guide semi-supervised fine-tuning, thereby fully exploiting the strengths of both paradigms.

Recent efforts have explored integrating these two paradigms by leveraging pre-trained models to extract domain knowledge from unlabeled data for downstream task adaptation. A common approach is model ensembling (Figure 1.a), such as V-PET (Gupte et al. 2024), which aggregates multi-view one-hot predictions from multiple vision models. As shown in Figure 1.b, another line of work selects top- k predictions using class-wise or confidence-based

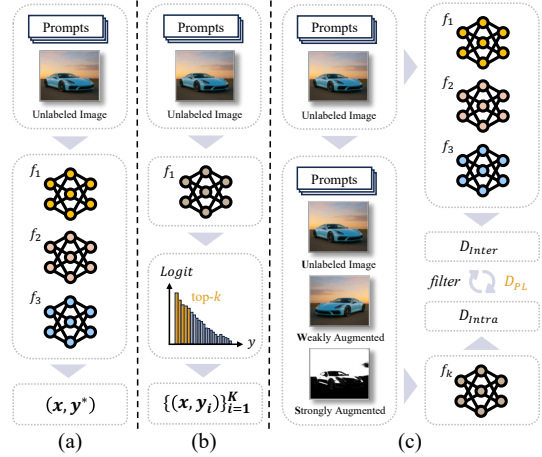


Figure 1: Comparison of existing pseudo-labeling paradigms and our proposed Bi-CoG. (a) Majority voting from multiple VLMs; (b) Top- k selection based on predicted logits; (c) Bi-CoG dynamically generate accurate and unbiased pseudo-labels based on bi-consistency and model error.

thresholds. For instance, GRIP (Menghini, Delworth, and Bach 2023) and UPL (Huang, Chu, and Wei 2022) enforce class balance by selecting equal samples per class; CPL (Zhang et al. 2024) refines labels via instance-level confidence matrices to reduce pre-training bias.

However, these methods struggle to balance the trade-off between pseudo-label accuracy and bias. Ensemble-based approaches can produce highly accurate pseudo-labels, but they often inadvertently amplify biases inherited from pre-training, leading to uneven performance across subgroups—a phenomenon commonly referred to as the “Matthew effect” (Zhu, Luo, and Liu 2022; Chen et al. 2022; Gan and Wei 2024). In contrast, soft-labeling techniques and class-wise pseudo-label allocation strategies can alleviate overconfidence to some extent, but they tend to introduce additional label noise and are highly sensitive to manually tuned hyperparameters. To the best of our knowledge, adaptively generating reliable and unbiased pseudo-labels in response to model performance remains a critical yet under-

*Corresponding author.

explored challenge in semi-supervised fine-tuning.

To address this challenge, we propose a novel method named **Bi-Consistency-Guided Self-Training (Bi-CoG)**. As illustrated in Figure 1.c, Bi-CoG leverages multiple VLMs as base learners to perform dynamic self-training guided by both inter- and intra-model consistency as well as model error estimation. Specifically, we conduct a dynamic self-training process that comprises three-stage pseudo-label selection. In the first stage, we apply majority voting to generate ensembled pseudo-labels, ensuring reliable supervision. Then, we assess each model’s bias on a sample using weak and strong augmentations: predictions consistent under no and weak augmentation but changing under strong augmentation indicate reliability and less prone to pre-training bias. Finally, based on theoretical insights, we dynamically adjust the upper bound on the number of pseudo-labels used for training, according to models’ relative accuracy on labeled data. This further filters pseudo-labels and enables adaptive self-training throughout the training process.

As a plug-and-play approach, Bi-CoG can be seamlessly integrated into existing VLM fine-tuning pipelines. To evaluate its effectiveness, we conduct experiments under both *open-world generalization* (Zhou et al. 2024) and *standard semi-supervised learning* (Yang et al. 2022) settings, combining Bi-CoG with various prompt-tuning methods. Extensive results demonstrate the effectiveness of our bi-consistency-guided dynamic self-training strategy, which consistently improves performance across 14 datasets without relying on larger models or external knowledge, outperforming state-of-the-art (SOTA) methods.

Our main contributions are summarized as follows:

- We propose Bi-CoG, a plug-and-play method that jointly leverages the pre-trained knowledge of VLMs and external information from unlabeled data.
- We design a deeply coupled self-training strategy integrates inter-model consistency, intra-model consistency and model error estimation, enabling reliable, low-bias pseudo-label generation and adaptive training.
- Theoretical analysis and extensive experiments demonstrate that Bi-CoG consistently improves performance, achieving up to a 5.69% gain across 14 datasets and surpassing SOTA methods.

Related Work

Parameter-efficient Fine-tuning on VLMs While pre-trained VLMs demonstrate strong zero-shot generalization in domain-specific downstream tasks, their large parameter sizes often hinder efficient adaptation to specific applications (Zhou et al. 2022b). To address this, recent works have proposed parameter-efficient fine-tuning approaches that introduce a small number of trainable parameters while keeping the majority of the model frozen (Li et al. 2024). Tip-Adapter (Zhang et al. 2022) and CLIP-Adapter (Gao et al. 2024) append lightweight bottleneck layers after the text or image encoders to learn residual features for better representation. CoOp (Zhou et al. 2022b) introduces prompt tuning to VLMs for the first time by replacing manually crafted hard prompts (e.g., “a photo of a classname”) with learnable

soft text prompts optimized via backpropagation. Building on this idea, methods such as MaPLe (Khattak et al. 2023a), PromptSRC (Khattak et al. 2023b), and BMIP (Lv et al. 2025a) extend prompt tuning to both visual and textual encoders, enabling joint vision-language adaptation. While these methods have advanced the application of VLMs to downstream tasks, the transformation of prompts into continuous vectors makes them prone to overfitting and leads to sub-optimal performance in open-world scenarios (Zhou et al. 2022a; Khattak et al. 2023b).

Pseudo-labeling in Semi-supervised Learning Semi-supervised learning (SSL) addresses label scarcity by leveraging both labeled and unlabeled data. Pseudo-labeling, the most widely used SSL approach, assigns labels to unlabeled data based on model predictions and improves performance through self-training. The key to effective pseudo-labeling lies in the generation of high-quality pseudo-labels (Yang et al. 2022). Traditional SSL methods typically filter pseudo-labels using confidence thresholds or adopt data augmentation to generate diverse views, aiming to improve label quality and model robustness (Lee et al. 2013a). For VLMs, their strong generalization ability allows them to produce highly accurate pseudo-labels even in zero- or few-shot settings, making them strong candidates as pseudo-labelers. Recent works have explored more advanced strategies: GRIP (Menghini, Delworth, and Bach 2023) gradually increases the upper limit on the number of pseudo-labels to mitigate calibration errors (Oh et al. 2024) and label imbalance (Wang et al. 2022); and CPL (Zhang et al. 2024) progressively refines pseudo-labels based on a confidence score matrix to avoid overconfidence. Despite their effectiveness, these methods struggle with balancing pseudo-label noise and inherited pre-training biases (Oh et al. 2024; Wang et al. 2022), while failing to dynamically adapt to model performance, ultimately limiting their potential.

Preliminary

In this section, we first revisit the core principles of CLIP (Radford et al. 2021), one of the most widely used VLMs, along with its associated prompt tuning methods, and subsequently formalize our problem definition.

CLIP. CLIP comprises a text encoder ψ and an image encoder ϕ , aligned via pretraining on massive image-text pairs. Given an image x and a set of class labels $\mathcal{Y} = y_1, \dots, y_C$, CLIP classifies x by computing the similarity between the image representation $z = \phi(x)$ and each class representation $w_i = \psi(\pi_i)$, where π_i is a natural language prompt such as "a photo of a [CLASS_{*i*}]". The predicted probability is computed as follows:

$$p(y = i | x) = \frac{\exp(\cos(\phi(x), \psi(w_i))/\tau)}{\sum_{j=1}^C \exp(\cos(\phi(x), \psi(w_j))/\tau)} \quad (1)$$

where τ is a temperature parameter that controls the sharpness of the probability distribution.

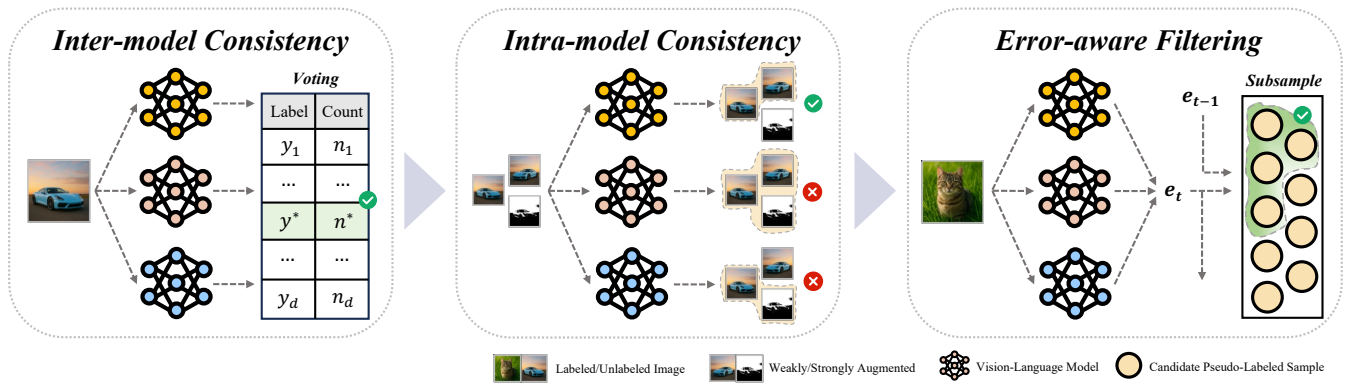


Figure 2: The overall framework of Bi-CoG’s pseudo-label selection. During the self-training phase, Bi-CoG employs inter-model consistency, intra-model consistency, and error-aware filtering to generate accurate and unbiased pseudo-labels, which are then used to fine-tune the target VLM.

Prompt Tuning. As a representative PEFT method for CLIP-based VLMs, prompt tuning learns adaptable prompts instead of fine-tuning the text encoder ψ . For instance, some studies (Zhou et al. 2022b,a) replace manually designed prompt templates with learnable prompt vectors $P = [t_1, t_2, \dots, t_n]$, where each t_i is a trainable token vector and n denotes the prompt length. Given a set of class names $[c_1, c_2, \dots, c_N]$, the prediction probability is computed as:

$$p(y = i | x) = \frac{\exp(\cos(\phi(x), \psi([P, c_i]))/\tau)}{\sum_{j=1}^N \exp(\cos(\phi(x), \psi([P, c_j]))/\tau)} \quad (2)$$

where $[\cdot, \cdot]$ denotes concatenation. The prompt P is optimized via backpropagation during fine-tuning.

Problem Definition. In downstream scenarios with scarce labeled data, we typically have access to a small labeled dataset denoted as $D_L = \{(x_i, y_i)\}_{i=1}^M$, along with a large amount of unlabeled data $D_{UL} = \{x_i\}_{i=1}^N$, where $M \ll N$. Given a collection of K pre-trained VLMs $\{f_k\}_{k=1}^K$ (with $K \geq 3$), the objective is to effectively leverage both D_L and D_{UL} to fine-tune the models and maximize performance on the target dataset D_{test} .

Methodology

To address the prevalent challenges of balancing pseudo-label accuracy with model bias and reducing the strong reliance on empirical parameter tuning in prior methods, we propose Bi-Consistency-Guided Self-Training (Bi-CoG), a simple yet effective plug-and-play framework. As illustrated in Figure 2, the Bi-CoG framework comprises the following three major components for pseudo-label selection:

- A model ensembling module that aggregates predictions through majority voting based on inter-model consistency, generating high-quality candidate pseudo-labels to ensure reliable supervision.
- A multi-view filtering mechanism that leverages intra-model consistency by applying diverse transformations to unlabeled data and discarding biased samples with inconsistent predictions, thereby mitigating the influence of pre-training bias.

- An error-aware bounding strategy that dynamically estimates model performance and sets an upper limit on the number of pseudo-labels used, promoting stable and progressive self-training.

The main procedure of Bi-CoG is summarized in Algorithm 1, and we elaborate on each component in the subsequent sections.

Inter-model Consistency

During self-training with pseudo-labeled data, label fidelity is critical to effective and stable optimization (Angluin and Laird 1988). Excessive noise can mislead learning, causing convergence to suboptimal or incorrect representations. To mitigate this issue, we first generate pseudo-labels based on inter-model consistency by integrating predictions of multiple VLMs, with the primary goal of ensuring the accuracy of pseudo-labels.

Concretely, for each model f_j ($1 \leq j \leq K$), we construct a candidate pseudo-labeled dataset D_{Inter}^j by selecting unlabeled instances on which the majority of the other $K - 1$ models reach a consensus. For each unlabeled sample $x_i \in D_{UL}$, we first compute the class-wise vote count from the other models as follows:

$$v_i(y) = \sum_{1 \leq k \leq K, k \neq j} \mathbb{I}[f_k(x_i) = y] \quad (3)$$

If the most voted label $y^* = \arg \max_{y \in \mathcal{Y}} v_i(y)$ satisfies $v_i(y^*) \geq \lceil \frac{K-1}{2} \rceil$, we assign x_i a pseudo-label $\hat{y}_i = y^*$ and include the pair (x_i, y^*) in D_{Inter}^j . Otherwise, the sample is discarded. Formally, this candidate set is defined as:

$$D_{Inter}^j = \left\{ (x_i, y^*) \mid v_i(y^*) \geq \left\lceil \frac{K-1}{2} \right\rceil \right\} \quad (4)$$

where \mathcal{Y} denotes the label space, and $\mathbb{I}[\cdot]$ is the indicator function. This inter-model consistency strategy ensembles multiple models to generate more reliable pseudo-labels, reducing noise from individual prediction errors. Moreover,

Algorithm 1: Bi-CoG’s overall learning algorithm.

Input: Pre-trained VLMs $\{f_k\}_{k=1}^K$, labeled data D_L , unlabeled data D_{UL} , scaling factor α
Output: Fine-tuned VLMs

- 1: **for** $j = 1$ **to** K **do**
- 2: $e'_j \leftarrow 0.5$, $\text{update}_j \leftarrow \text{False}$
- 3: **end for**
- 4: $t \leftarrow 0$, $\text{improve} \leftarrow \text{True}$
- 5: **while** improve **do**
- 6: $t \leftarrow t + 1$
- 7: **for** $j = 1$ **to** K **do**
- 8: $\text{update}_j \leftarrow \text{False}$
- 9: $e_j \leftarrow \text{MeasureError}(D_L, \{f_k\}_{k \neq j}^K)$
- 10: **if** $e_j < e'_j$ **then**
- 11: $D_{Inter}^j \leftarrow \text{InterConsistency}(D_{UL}, \{f_k\}_{k \neq j}^K)$
- 12: $D_{Intra}^j \leftarrow \text{IntraConsistency}(D_{UL}, \{f_k\}_{k \neq j}^K)$
- 13: $\text{update}_j \leftarrow \text{ErrorAware}(e_j, e'_j, t)$
- 14: $D_{PL}^j \leftarrow \text{Subsample}(D_{Inter}^j \cap D_{Intra}^j, (\frac{e'_j}{e_j})^{\alpha t} L_j')$
- 15: **end if**
- 16: **if** update_j **then**
- 17: $e'_j \leftarrow e_j$, $f_j \leftarrow \text{FineTune}(f_j, D_L \cup D_{PL}^j)$
- 18: **end if**
- 19: **end for**
- 20: **if** $\text{update} == [\text{False}] * K$ **then**
- 21: $\text{improve} \leftarrow \text{False}$
- 22: **end if**
- 23: **end while**
- 24: **return** $\{f_k\}_{k=1}^K$

the leave-one-out scheme prevent amplifying biases inherent to the target model, thereby resulting in more accurate and unbiased candidate datasets for fine-tuning.

Intra-model Consistency

While inter-model consistency improves pseudo-label reliability by aggregating agreement across models, it may still preserve instances where VLMs share similar biases, often due to overlapping pre-training corpora or architectural homogeneity (Gan and Wei 2024; Wang and Russakovsky 2023). To further mitigate biased supervision, we introduce intra-model consistency, which leverages the consistency of a single model’s predictions under different input views to refine the pseudo-labeled sets obtained in the previous stage.

Specifically, for each unlabeled sample $x_i \in D_{UL}$, we apply both weak and strong data augmentations. Each model f_k then produces predictions on the original input x_i , the weakly augmented \tilde{x}_i^w , and the strongly augmented \tilde{x}_i^s . A sample is retained only if the prediction remains consistent between the original and weakly augmented inputs, i.e., $f_k(x_i) = f_k(\tilde{x}_i^w)$, but differs under strong augmentation, i.e., $f_k(\tilde{x}_i^s) \neq f_k(x_i)$. This criterion identifies samples with low uncertainty and meaningful sensitivity, as evidenced by prediction consistency under weak perturbations and inconsistency under strong perturbations. The intra-model consistent pseudo-label set for f_j is defined as the intersection of predictions from the other models:

$$D_{Intra}^j = \bigcap_{\substack{k=1 \\ k \neq j}}^K \left\{ (x_i, f_k(x_i)) \mid \begin{array}{l} f_k(x_i) = f_k(\tilde{x}_i^w) \\ f_k(x_i) \neq f_k(\tilde{x}_i^s) \end{array} \right\} \quad (5)$$

Once the D_{Intra}^j are computed, the candidate pseudo-label set for target model f_j is constructed by intersecting its inter-model consistent set D_{Inter}^j with the intra-model consistent set :

$$D_{PL}^j = D_{Inter}^j \cap D_{Intra}^j \quad (6)$$

The intersection of pseudo-labels from inter- and intra-model consistency preserves accuracy while mitigating shared model biases. Consequently, the resulting pseudo-labeled datasets are both highly reliable and low in bias, providing a robust foundation for the subsequent dynamic self-training stage.

Error-aware Filtering

After bi-consistency-guided pseudo-labeling, we obtain a candidate sample set D_{PL} , which contains high-accuracy and low-biased pseudo-labels. However, during self-training, it is crucial to determine an appropriate upper bound on the number of pseudo-labeled samples based on model performance. Prior studies (Angluin and Laird 1988; Chen et al. 2022) have shown that even minor label noise, if not aligned with model competence, can significantly degrade performance, making further noise reduction in D_{PL} essential. Existing methods (Menghini, Delworth, and Bach 2023; Huang, Chu, and Wei 2022) typically rely on fixed thresholds to limit the number of pseudo-labels, which may be suboptimal as model performance evolves over time.

To address this limitation, we dynamically adjust the upper bound on pseudo-label usage based on estimated model error ratio, guided by a theoretical analysis. Specifically, following prior work (Angluin and Laird 1988; Zhou and Li 2005) we formalize the influence of noisy supervision on model f_j during iterative self-training:

Lemma 1. *Let L_t denote the training set D_{train} for model f_j at iteration t , and e_t represent the relative error rate of the remaining $K - 1$ models at the same iteration, i.e., the probability that the majority vote produces an incorrect label. Then, training f_j on D_{train} will result in performance improvement if the following condition is satisfied:*

$$0 < \frac{e_t}{e_{t-1}} < \frac{L_{t-1}}{L_t} < 1 \quad (7)$$

According to Lemma 1, the model will be improved throughout the training process as long as Equation 7 holds. In practice, we estimate the theoretical error rate ratio from the performance of the $K - 1$ models on the labeled set. However, this estimation can be biased, as repeated training on labeled data tends to produce stable—and often low—error ratios, which are reflected in Equation 7 as values close to 1. In contrast, the actual error ratio on unlabeled

Method	Average		ImageNet		Caltech101		OxfordPets		StanfordCars	
	HM	Acc.	HM	Acc.	HM	Acc.	HM	Acc.	HM	Acc.
CLIP	73.00	66.41	70.18	66.70	95.68	93.30	94.11	89.10	68.85	65.60
CoOp	72.10	66.59	72.00 \pm 0.34	68.73 \pm 0.25	90.91 \pm 1.61	89.90 \pm 0.99	93.97 \pm 0.72	88.73 \pm 0.09	69.94 \pm 0.59	66.40 \pm 0.50
+ Bi-CoG	77.79	71.03	73.06 \pm 0.08	69.78 \pm 0.04	96.67 \pm 0.05	94.24 \pm 0.25	96.28 \pm 0.60	89.57 \pm 2.02	73.38 \pm 0.31	69.31 \pm 0.76
MaPLe	78.78	72.18	73.58 \pm 0.09	70.30 \pm 0.14	96.58 \pm 0.21	94.87 \pm 0.09	96.60 \pm 0.36	92.33 \pm 0.31	73.53 \pm 0.81	69.97 \pm 0.87
+ Bi-CoG	79.77	73.54	74.11 \pm 0.07	70.82 \pm 0.09	96.77 \pm 0.17	95.09 \pm 0.46	96.93 \pm 0.06	92.56 \pm 0.12	74.20 \pm 0.31	70.48 \pm 0.36
PromptSRC	79.99	74.11	74.07 \pm 0.06	70.77 \pm 0.05	96.11 \pm 0.08	94.63 \pm 0.12	96.26 \pm 0.29	92.13 \pm 0.59	76.68 \pm 0.16	73.03 \pm 0.19
+ Bi-CoG	81.46	74.96	74.18 \pm 0.03	70.94 \pm 0.03	96.45 \pm 0.16	94.74 \pm 0.16	96.37 \pm 0.13	92.62 \pm 0.13	79.07 \pm 0.15	73.77 \pm 0.01

Method	Flowers102		Food101		FGVCAircraft		SUN397		DTD	
	HM	Acc.								
CLIP	74.44	70.70	90.39	85.60	31.21	24.80	72.37	62.60	56.62	44.00
CoOp	75.70 \pm 2.82	71.27 \pm 2.21	85.82 \pm 1.41	80.03 \pm 1.17	29.93 \pm 1.54	26.07 \pm 0.74	71.60 \pm 1.81	63.33 \pm 1.44	55.93 \pm 1.25	50.87 \pm 0.62
+ Bi-CoG	83.57 \pm 0.91	79.59 \pm 1.22	90.54 \pm 0.14	85.03 \pm 0.65	35.61 \pm 0.29	28.40 \pm 0.21	76.89 \pm 0.06	67.15 \pm 0.18	59.90 \pm 1.37	50.96 \pm 1.35
MaPLe	82.98 \pm 0.19	78.47 \pm 0.60	90.83 \pm 0.35	86.47 \pm 0.40	35.30 \pm 0.88	27.30 \pm 0.96	79.42 \pm 0.30	70.97 \pm 0.24	67.40 \pm 3.09	55.30 \pm 1.40
+ Bi-CoG	84.62 \pm 0.25	79.12 \pm 0.51	91.67 \pm 0.03	87.46 \pm 0.02	35.58 \pm 0.71	27.63 \pm 0.56	80.27 \pm 0.19	71.82 \pm 0.23	69.88 \pm 1.07	56.36 \pm 0.73
PromptSRC	86.13 \pm 0.39	80.77 \pm 0.50	90.91 \pm 0.12	86.47 \pm 0.12	34.99 \pm 6.68	29.93 \pm 2.50	80.68 \pm 0.23	72.13 \pm 0.26	70.72 \pm 1.23	58.87 \pm 1.28
+ Bi-CoG	87.60 \pm 0.18	83.19 \pm 0.55	91.25 \pm 0.01	86.65 \pm 0.02	39.89 \pm 0.34	31.98 \pm 0.69	80.89 \pm 0.04	72.43 \pm 0.10	71.67 \pm 0.42	59.48 \pm 0.10

Method	EuroSAT		UCF101		CIFAR-10		CIFAR-100		ImageNet-100	
	HM	Acc.								
CLIP	60.21	48.30	74.42	67.50	88.43	79.00	55.17	46.00	88.33	86.50
CoOp	72.04 \pm 3.29	59.50 \pm 2.10	67.03 \pm 1.48	64.23 \pm 1.26	89.17 \pm 1.32	77.00 \pm 2.42	53.42 \pm 3.23	45.03 \pm 2.88	81.97 \pm 2.38	81.17 \pm 1.96
+ Bi-CoG	85.84 \pm 1.98	67.98 \pm 0.67	73.11 \pm 1.99	68.01 \pm 0.92	92.07 \pm 0.46	82.28 \pm 0.99	61.71 \pm 0.26	52.55 \pm 0.32	90.39 \pm 0.35	89.59 \pm 0.30
MaPLe	78.35 \pm 1.46	60.90 \pm 8.71	81.57 \pm 0.39	74.70 \pm 0.57	92.02 \pm 0.76	83.83 \pm 1.21	64.73 \pm 0.30	56.10 \pm 0.37	90.00 \pm 0.17	89.07 \pm 0.33
+ Bi-CoG	81.33 \pm 2.89	70.52 \pm 2.81	82.23 \pm 0.58	75.75 \pm 0.51	92.15 \pm 0.09	84.41 \pm 0.69	66.68 \pm 0.52	57.97 \pm 0.61	90.41 \pm 0.29	89.52 \pm 0.32
PromptSRC	81.87 \pm 2.52	70.03 \pm 0.86	82.30 \pm 0.87	76.67 \pm 0.37	91.46 \pm 0.30	83.80 \pm 0.42	67.23 \pm 0.42	58.93 \pm 0.39	90.49 \pm 0.22	89.43 \pm 0.26
+ Bi-CoG	86.28 \pm 0.87	71.01 \pm 0.47	83.09 \pm 0.24	77.30 \pm 0.44	94.50 \pm 0.15	84.96 \pm 1.75	68.19 \pm 0.38	60.20 \pm 0.07	91.07 \pm 0.02	90.15 \pm 0.05

Table 1: Performance comparison on 14 datasets using ViT-B/16 architecture. The best performance is in bold.

data typically decreases during training, making the true ratio $\frac{\hat{e}_t}{\hat{e}_{t-1}}$ lower than the estimated $\frac{e_t}{e_{t-1}}$. Ignoring this discrepancy would introduce bias into the estimated pseudo-label budget, compromising the validity of the theoretical analysis. To address this issue, we introduce Theorem 1 to provide a correction:

Theorem 1. *As the training progresses, the true error rate ratio can be approximately equal to the t -power of the estimated error rate ratio, as shown below:*

$$\frac{e_t}{e_{t-1}} \approx \left[\frac{\hat{e}_t}{\hat{e}_{t-1}} \right]^{\alpha t} \quad (8)$$

where $\alpha > 0$ is a scaling factor that reflects the error reduction rate. Then, the original condition in Equation 7 is approximately equivalent to the following constraints:

$$L_t \leq \left[\left(\frac{\hat{e}_{t-1}}{\hat{e}_t} \right)^{\alpha t} \times L_{t-1} - 1 \right] \quad (9)$$

$$L_{t-1} > \frac{\hat{e}_t^{\alpha t}}{\hat{e}_{t-1}^{\alpha t} - \hat{e}_t^{\alpha t}}$$

A detailed proof of Lemma 1 and Theorem 1 is provided in the supplementary material. Based on the theoretical analysis, we establish the necessary condition under which the model can be effectively optimized by self-training, as described in Equation 9, and establish an upper bound on the pseudo-label budget for each iteration. Accordingly, the final set of pseudo-labeled samples is formalized as:

$$D_{PL}^j = \text{Subsample} \left(D_{PL}^j, \left(\frac{e'_j}{e_j} \right)^{\alpha t} L'_j \right) \quad (10)$$

This dynamic filtering strategy reduces the mismatch between model capacity and pseudo-label quantity. Consequently, the model can self-regulate the amount of pseudo-labeled data during training, leading to stable and consistent performance improvements.

In summary, Bi-CoG' offers the following advantages:

- Plug-and-Play Adaptability:** Bi-CoG can be seamlessly integrated into existing pretrain-finetune pipelines, providing consistent performance improvements with minimal changes to the original framework.
- Robust Pseudo-Labeling:** By jointly leveraging bi-consistency and error-aware mechanisms, Bi-CoG gen-

erates more reliable pseudo-labels, effectively reducing label noise and alleviating model bias.

3. **Adaptive Self-Training Control:** Empowered by the error-aware mechanism, Bi-CoG can automatically regulate the self-training process, eliminating the need for manually preset iteration counts and enhances adaptability across different scenarios.

Experiment

In this section, we design experiments to answer the following research questions:

1. **RQ1:** Does Bi-CoG enhance existing PEFT methods for VLMs in open-world generalization scenarios?
2. **RQ2:** Can Bi-CoG deliver competitive performance compared to conventional SSL approaches?
3. **RQ3:** How does Bi-CoG compare to other methods that jointly leverage pre-trained models and unlabeled data?
4. **RQ4:** What is the contribution of each component within the Bi-CoG framework?

Experimental Settings

Evaluation Paradigm. To answer RQ1 and RQ2, we evaluate the effectiveness of Bi-CoG on two widely adopted settings: *open-world generation setting* (Zhou et al. 2024; Lv et al. 2025a) and *semi-supervised setting* (Lee et al. 2013b; Yang et al. 2022). In *open-world generation setting*, the model is trained only on a subset of categories (referred to as base classes), while the remaining categories are treated as novel classes. We report the harmonic mean (HM) of the model’s performance on base and novel classes, as well as the overall accuracy on the full test set, which includes both base and novel classes. *Semi-supervised setting* follows a common protocol where only a small portion of the data is labeled, while the majority remains unlabeled.

Dataset and Baselines. We evaluate the performance of our method on 14 recognition datasets, including 11 commonly used for assessing VLMs and 3 classical benchmarks for semi-supervised learning. Detailed information about the datasets is provided in the supplementary material. We select CLIP (Radford et al. 2021) and its three representative prompt tuning methods as baselines: CoOp (Zhou et al. 2022b), MaPLe (Khattak et al. 2023a), and PromptSRC (Khattak et al. 2023b), among which PromptSRC represents the current SOTA method. For methods that integrate the two paradigms, we select GRIP (Menghini, Delworth, and Bach 2023) and CPL (Zhang et al. 2024) as baselines, with CPL representing the current SOTA approach. The parameters of Bi-CoG and additional experimental details are provided in the supplementary material.

Experimental Results

RQ1: Does Bi-CoG enhance existing PEFT methods for VLMs in open-world generalization scenarios?

To evaluate the robustness of Bi-CoG in open-world scenarios, we conduct a comprehensive study by integrating it with three representative prompt tuning methods across 14

Method	CIFAR-10		CIFAR-100	
	4 shots	25 shots	4 shots	25 shots
ReMixMatch	80.90 \pm 9.64	94.56 \pm 0.05	55.72 \pm 2.06	72.57 \pm 0.31
FixMatch (RA)	86.19 \pm 3.37	94.93 \pm 0.65	51.15 \pm 1.75	71.71 \pm 0.11
FixMatch (CTA)	88.61 \pm 3.35	94.93 \pm 0.33	50.05 \pm 3.01	71.36 \pm 0.24
CoOp	80.60 \pm 1.79	85.10 \pm 0.29	49.00 \pm 0.83	57.43 \pm 0.25
+ <i>Bi-CoG</i>	84.90 \pm 1.06	86.10 \pm 0.03	52.77 \pm 0.24	58.05 \pm 0.05
PromptSRC	86.03 \pm 0.48	90.10 \pm 0.08	60.33 \pm 0.17	66.33 \pm 0.29
+ <i>Bi-CoG</i>	89.83 \pm 0.35	91.07 \pm 0.42	60.56 \pm 0.79	66.84 \pm 0.67

Table 2: Performance on low-resolution SSL datasets.

datasets. For each dataset, we report two metrics: HM of base and novel class accuracies, and overall accuracy (Acc.). We set the base-to-novel class ratio to 50:50 and report the mean and standard deviation over three runs. As shown in Table 1, Bi-CoG consistently improves both metrics across all datasets, achieving the highest average performance. Notably, when applied to CoOp, Bi-CoG yields over a 5% improvement in HM. Moreover, Bi-CoG demonstrates particularly strong gains on traditional open-world benchmarks. For example, on low-resolution datasets such as CIFAR-10 and CIFAR-100 (Krizhevsky, Hinton et al. 2009), it achieves up to an 8% increase in HM, underscoring its effectiveness across datasets with varying resolutions. These results highlight the effectiveness of Bi-CoG and emphasize the importance of integrating unsupervised strategies with pre-trained models for improved generalization in open-world settings.

RQ2: Can Bi-CoG deliver competitive performance compared to conventional SSL approaches?

As shown in Table 2, SSL algorithms exhibit a significant advantage over baseline prompt tuning methods on SSL datasets. This is largely due to the lower resolution of these datasets, which makes it more difficult for VLMs to effectively capture visual content (Krizhevsky, Hinton et al. 2009; Lv et al. 2025b). This limitation is also reflected in the sensitivity to the number of shots: increasing the number of shots from 4 to 25 yields much larger performance gains for SSL algorithms compared to VLM-based prompt tuning. However, Bi-CoG provides the model with more reliable training examples, enabling prompt tuning methods to achieve SOTA performance under the challenging 4-shot setting.

These results demonstrate that Bi-CoG can effectively leverage unlabeled data to capture richer visual representations, even in low-resolution and data-scarce scenarios.

RQ3: How does Bi-CoG compare to other methods that jointly leverage pre-trained models and unlabeled data?

To further validate the effectiveness of Bi-CoG, we conducted comparative experiments against the current SOTA methods GRIP (Menghini, Delworth, and Bach 2023) and CPL (Zhang et al. 2024) on the Flowers102 dataset (Nilsback and Zisserman 2008). Following GRIP, we adopt the same base-to-novel class ratio of 62:38, and use CoOp as the underlying prompt tuning method for Bi-CoG and other

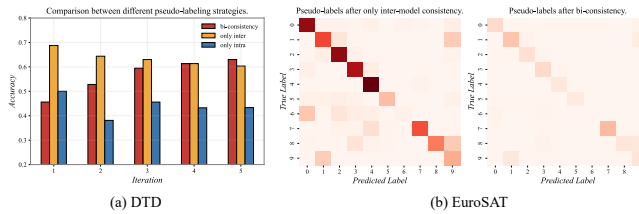


Figure 3: (a) Pseudo-label accuracy over training iterations on the DTD dataset under different pseudo-labeling strategies; (b) Distribution of pseudo-labels on the EuroSAT dataset before and after applying the intra-model consistency.

approaches to ensure fairness. As shown in Table 3, our Bi-CoG achieves the best performance under both settings, outperforming CPL by up to 5.9 percentage points in SSL setting. More importantly, Bi-CoG eliminates the need for manually setting hyperparameters such as the number of pseudo-labels k , effectively decreasing the reliance on manual tuning and susceptibility to internal model bias.

In summary, Bi-CoG represents one of the most effective integrations of pretrain-finetuning and SSL methods to date.

Ablation Study

To answer **RQ4**, we first examine the impact of the bi-consistency-guided pseudo-labeling strategy on both pseudo-label accuracy and the distribution of biased samples. As shown in Figure 3.a, removing the inter-model consistency module results in a notable decline in pseudo-label accuracy, highlighting the importance of ensemble-based labeling for generating high-quality supervision. Notably, although the bi-consistency strategy exhibits relatively lower pseudo-label accuracy in the early stages of training, its accuracy steadily improves as training progresses. In contrast, other single-strategy pseudo-labeling methods show either a decline or fluctuation in accuracy, demonstrating the stability and reliability of bi-consistency-guided pseudo-labeling. Furthermore, as illustrated in Figure 3.b, incorporating intra-model consistency helps smooth the class-wise distribution of pseudo-labels, effectively mitigating the bias inherited from pre-training. These results collectively confirm that the bi-consistency-guided strategy produces pseudo-labels that are both more accurate and less biased—two critical factors for stable and effective self-training.

To further validate the theoretical foundation of our error-aware mechanism, we analyze the evolution of the actual error rate ratio on pseudo-labeled samples and its estimation from labeled data on the StanfordCars dataset (Krause et al. 2013). As illustrated in Figure 4, the condition in Equation 8 holds reliably during training, supporting the practical validity of our theoretical derivation and confirming the soundness of the Bi-CoG’ dynamic self-training framework.

Finally, we conduct a comprehensive ablation study on the key components of Bi-CoG, using CoOp as the underlying prompt tuning method and reporting the average performance across 14 datasets. As shown in Table 4, any component of our three-stage pseudo-labeling strategy, which inte-

Method	Domain Data	SSL	Open-World
CLIP	Zero-shot	72.08	77.80
FPL		75.96	80.97
IFPL	Few-shot	78.68	82.08
GRIP	+ Unlabeled	83.60	86.26
CPL		89.66	87.35
Bi-CoG		96.45	88.01
Δ		+6.79	+0.66

Table 3: Performance comparison on the Flowers102 dataset, with a base-to-novel class ratio of 62:38. Our method outperforms prior approaches under both settings.

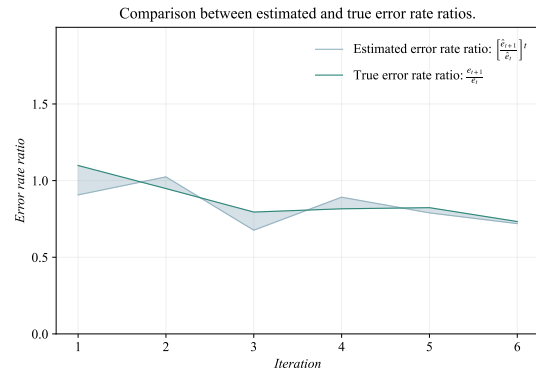


Figure 4: Comparison between the estimated and true error rate ratios on StanfordCars under the open-world setting. The scaling factor is fixed at $\alpha = 1$ throughout training.

grats bi-consistency and error-aware filtering, plays a critical role in improving model performance. This highlights the deeply coupled and effective design of the pseudo-labeling mechanism in Bi-CoG.

Conclusion

This paper investigates the integration of pre-trained vision-language models with semi-supervised learning for downstream tasks with sparse labeled data. We identify several critical issues in existing approaches, including the trade-off between label quality and model bias, as well as the limited adaptability arising from the reliance on manually set fixed thresholds. To address these challenges, we propose Bi-CoG, a plug-and-play self-training framework that incorporates a three-stage, deeply coupled pseudo-labeling strategy with adaptive adjustment capabilities. Theoretical analysis and experimental results across 14 datasets in both open-world generalization and semi-supervised settings demonstrate that Bi-CoG can be seamlessly integrated with any pretrain-finetuning methods, consistently achieving performance improvements.

Method	Open-World	
	HM	Acc.
CoOp + Bi-CoG	77.79	71.03
- w/o. Inter-model consistency	76.14	68.83
- w/o. Intra-model consistency	75.85	69.08
- w/o. Error-aware filtering	76.92	70.92

Table 4: Ablation study of Bi-CoG’s pseudo-labeling strategy under the open-world generalization setting. Experimental results show that each component plays a critical role in improving model performance.

References

Angluin, D.; and Laird, P. 1988. Learning from noisy examples. *Machine learning*, 2(4): 343–370.

Bossard, L.; Guillaumin, M.; and Van Gool, L. 2014. Food-101 - Mining Discriminative Components with Random Forests. In *Proceedings of the 13th European Conference on Computer Vision*, 446–461.

Chen, B.; Jiang, J.; Wang, X.; Wan, P.; Wang, J.; and Long, M. 2022. Debaised self-training for semi-supervised learning. *Advances in Neural Information Processing Systems*, 35: 32424–32437.

Cimpoi, M.; Maji, S.; Kokkinos, I.; Mohamed, S.; and Vedaldi, A. 2014. Describing Textures in the Wild. In *Proceedings of the 2014 IEEE Conference on Computer Vision and Pattern Recognition*, 3606–3613.

Deng, J.; Dong, W.; Socher, R.; Li, L.-J.; Li, K.; and Fei-Fei, L. 2009. ImageNet: a large-scale hierarchical image database. In *Proceedings of the 2009 IEEE Conference on Computer Vision and Pattern Recognition*, 248–255.

Fei-Fei, L.; Fergus, R.; and Perona, P. 2004. Learning Generative Visual Models from Few Training Examples: An Incremental Bayesian Approach Tested on 101 Object Categories. In *the 2004 IEEE Conference on Computer Vision and Pattern Recognition Workshops*, 178.

Gan, K.; and Wei, T. 2024. Erasing the Bias: Fine-Tuning Foundation Models for Semi-Supervised Learning. In Salakhutdinov, R.; Kolter, Z.; Heller, K.; Weller, A.; Oliver, N.; Scarlett, J.; and Berkenkamp, F., eds., *Proceedings of the 41st International Conference on Machine Learning*, volume 235 of *Proceedings of Machine Learning Research*, 14453–14470. PMLR.

Gao, P.; Geng, S.; Zhang, R.; Ma, T.; Fang, R.; Zhang, Y.; Li, H.; and Qiao, Y. 2024. Clip-adapter: Better vision-language models with feature adapters. *International Journal of Computer Vision*, 132(2): 581–595.

Gupte, S. R.; Aklilu, J.; Nirschl, J. J.; and Yeung-Levy, S. 2024. Revisiting Active Learning in the Era of Vision Foundation Models. *Transactions on Machine Learning Research*.

Helber, P.; Bischke, B.; Dengel, A.; and Borth, D. 2019. EuroSAT: a novel dataset and deep learning benchmark for land use and land cover classification. *IEEE Journal of Selected*

Topics in Applied Earth Observations and Remote Sensing, 2217–2226.

Huang, T.; Chu, J.; and Wei, F. 2022. Unsupervised prompt learning for vision-language models. *arXiv preprint arXiv:2204.03649*.

Jia, C.; Yang, Y.; Xia, Y.; Chen, Y.-T.; Parekh, Z.; Pham, H.; Le, Q.; Sung, Y.-H.; Li, Z.; and Duerig, T. 2021. Scaling up visual and vision-language representation learning with noisy text supervision. In *International conference on machine learning*, 4904–4916. PMLR.

Khattak, M. U.; Rasheed, H.; Maaz, M.; Khan, S.; and Khan, F. S. 2023a. Maple: Multi-modal prompt learning. In *Proceedings of the IEEE/CVF conference on computer vision and pattern recognition*, 19113–19122.

Khattak, M. U.; Wasim, S. T.; Naseer, M.; Khan, S.; Yang, M.-H.; and Khan, F. S. 2023b. Self-regulating prompts: Foundational model adaptation without forgetting. In *Proceedings of the IEEE/CVF international conference on computer vision*, 15190–15200.

Krause, J.; Stark, M.; Deng, J.; and Fei-Fei, L. 2013. 3D object representations for fine-grained categorization. In *the 2013 IEEE International Conference on Computer Vision Workshops*, 554–561.

Krizhevsky, A.; Hinton, G.; et al. 2009. Learning multiple layers of features from tiny images.

Lee, D.-H.; et al. 2013a. Pseudo-label: The simple and efficient semi-supervised learning method for deep neural networks. In *Workshop on challenges in representation learning, ICML*, volume 3, 896. Atlanta.

Lee, D.-H.; et al. 2013b. Pseudo-label: The simple and efficient semi-supervised learning method for deep neural networks. In *Workshop on challenges in representation learning, ICML*, 896.

Li, M.; Zhong, J.; Li, C.; Li, L.; Lin, N.; and Sugiyama, M. 2024. Vision-Language Model Fine-Tuning via Simple Parameter-Efficient Modification. In Al-Onaizan, Y.; Bansal, M.; and Chen, Y.-N., eds., *Proceedings of the 2024 Conference on Empirical Methods in Natural Language Processing*, 14394–14410. Miami, Florida, USA: Association for Computational Linguistics.

Lv, S.-L.; Chen, Y.-Y.; Zhou, Z.; Yang, M.; and Guo, L.-Z. 2025a. BMIP: Bi-directional Modality Interaction Prompt Learning for VLM. *arXiv preprint arXiv:2501.07769*.

Lv, S.-L.; Zhu, R.; Li, Y.-F.; and Guo, L.-Z. 2025b. Unlabeled Data or Pre-trained Model: Rethinking Semi-Supervised Learning and Pretrain-Finetuning. *arXiv preprint arXiv:2505.13317*.

Maji, S.; Rahtu, E.; Kannala, J.; Blaschko, M.; and Vedaldi, A. 2023. Fine-grained visual classification of aircraft. arXiv:arXiv:1306.5151.

Menghini, C.; Delworth, A.; and Bach, S. 2023. Enhancing CLIP with CLIP: Exploring Pseudolabeling for Limited-Label Prompt Tuning. In Oh, A.; Naumann, T.; Globerson, A.; Saenko, K.; Hardt, M.; and Levine, S., eds., *Advances in Neural Information Processing Systems*, volume 36, 60984–61007. Curran Associates, Inc.

- Nilsback, M.-E.; and Zisserman, A. 2008. Automated flower classification over a large number of classes. In *Proceedings of the 6th Indian Conference on Computer Vision*, 722–729.
- Oh, C.; Lim, H.; Kim, M.; Han, D.; Yun, S.; Choo, J.; Hauptmann, A.; Cheng, Z.-Q.; and Song, K. 2024. Towards calibrated robust fine-tuning of vision-language models. *Advances in Neural Information Processing Systems*, 37: 12677–12707.
- Parkhi, O. M.; Vedaldi, A.; Zisserman, A.; and Jawahar, C. 2012. Cats and dogs. In *Proceedings of the 2012 IEEE Conference on Computer Vision and Pattern Recognition*, 3498–3505.
- Radford, A.; Kim, J. W.; Hallacy, C.; Ramesh, A.; Goh, G.; Agarwal, S.; Sastry, G.; Askell, A.; Mishkin, P.; Clark, J.; et al. 2021. Learning transferable visual models from natural language supervision. In *International conference on machine learning*, 8748–8763. PmLR.
- Sohn, K.; Berthelot, D.; Carlini, N.; Zhang, Z.; Zhang, H.; Raffel, C. A.; Cubuk, E. D.; Kurakin, A.; and Li, C.-L. 2020. Fixmatch: Simplifying semi-supervised learning with consistency and confidence. *Advances in neural information processing systems*, 596–608.
- Soomro, K.; Zamir, A. R.; and Shah, M. 2012. UCF101: A dataset of 101 human actions classes from videos in the wild. arXiv:arXiv:1212.0402.
- Wang, A.; and Russakovsky, O. 2023. Overwriting pre-trained bias with finetuning data. In *Proceedings of the IEEE/CVF international conference on computer vision*, 3957–3968.
- Wang, X.; Wu, Z.; Lian, L.; and Yu, S. X. 2022. Debaised learning from naturally imbalanced pseudo-labels. In *Proceedings of the IEEE/CVF Conference on Computer Vision and Pattern Recognition*, 14647–14657.
- Xiao, J.; Hays, J.; Ehinger, K. A.; Oliva, A.; and Torralba, A. 2010. Sun database: Large-scale scene recognition from abbey to zoo. In *Proceedings of the 2010 IEEE Conference on Computer Vision and Pattern Recognition*, 3485–3492.
- Yang, X.; Song, Z.; King, I.; and Xu, Z. 2022. A survey on deep semi-supervised learning. *IEEE transactions on knowledge and data engineering*, 35(9): 8934–8954.
- Zhang, J.; Wei, Q.; Liu, F.; and Feng, L. 2024. Candidate Pseudolabel Learning: Enhancing Vision-Language Models by Prompt Tuning with Unlabeled Data. In *Forty-First International Conference on Machine Learning*.
- Zhang, R.; Zhang, W.; Fang, R.; Gao, P.; Li, K.; Dai, J.; Qiao, Y.; and Li, H. 2022. Tip-Adapter: Training-Free Adaption of CLIP for Few-Shot Classification. In *Computer Vision – ECCV 2022: 17th European Conference, Tel Aviv, Israel, October 23–27, 2022, Proceedings, Part XXXV*, 493–510. Berlin, Heidelberg: Springer-Verlag. ISBN 978-3-031-19832-8.
- Zhou, K.; Yang, J.; Loy, C. C.; and Liu, Z. 2022a. Conditional prompt learning for vision-language models. In *Proceedings of the IEEE/CVF conference on computer vision and pattern recognition*, 16816–16825.
- Zhou, K.; Yang, J.; Loy, C. C.; and Liu, Z. 2022b. Learning to prompt for vision-language models. *International Journal of Computer Vision*, 130(9): 2337–2348.
- Zhou, Z.; Yang, M.; Shi, J.-X.; Guo, L.-Z.; and Li, Y.-F. 2024. DeCoOp: Robust Prompt Tuning with Out-of-Distribution Detection. In *Proceedings of the 41st International Conference on Machine Learning*.
- Zhou, Z.-H.; and Li, M. 2005. Tri-training: exploiting unlabeled data using three classifiers. *IEEE Transactions on Knowledge and Data Engineering*, 17(11): 1529–1541.
- Zhu, Z.; Luo, T.; and Liu, Y. 2022. The Rich Get Richer: Disparate Impact of Semi-Supervised Learning. In *International Conference on Learning Representations*.

Supplementary Material

A. Detailed Theoretical Analysis

A.1. Proof of Lemma 1

Proof. When the aggregated training data contains noisy samples, let \mathcal{F} denote the hypothesis space, η the noise ratio in the training set ($\eta < 0.5$), $\epsilon > 0$ the target error rate, and $\delta < 1$ the confidence parameter. According to PAC learning theory (Angluin and Laird 1988; Zhou and Li 2005), if the number of training samples m satisfies

$$m \geq \frac{2}{\epsilon^2(1-2\eta)^2} \ln \left(\frac{2|\mathcal{F}|}{\delta} \right), \quad (11)$$

then, for the learned model f and the optimal model f^* within \mathcal{F} , we have

$$\mathbb{P}[d(f, f^*) \geq \epsilon] \leq \delta, \quad (12)$$

where $d(f, f^*)$ denotes the excess error rate of f over f^* .

Let $c = 2\mu \ln \left(\frac{2|\mathcal{F}|}{\delta} \right)$, where μ makes is Eq. (11) hold equality. Eq. (11) can then be rewritten as

$$m = \frac{c}{\epsilon^2(1-2\eta)^2}. \quad (13)$$

Thus, the relationship between the error rate ϵ , the number of training samples m , and the noise ratio η is given by

$$\epsilon = \frac{\sqrt{c}}{\sqrt{m(1-2\eta)^2}}. \quad (14)$$

In the Bi-CoG training framework, we maintain K vision-language models (VLMs). Suppose our optimization target is the j -th model, denoted as f_j . We adopt the *leave-one-out* scheme and generate a pseudo-label candidate set D_{PL} using the remaining $K-1$ models via inter-model consistency and intra-model consistency. At iteration t , the candidate training set is

$$D_{train} = D_L \cup D_{PL}, \quad (15)$$

Let e_t be the probability that the prediction obtained by a majority vote (agreed upon by more than half of the $K-1$ models) is still incorrect. Denote $|D_L| = L$ and $|D_{PL}| = L_t$, and approximate $|D_{train}| \approx L + L_t$. The noise ratio at iteration t is then estimated as

$$\eta_t = \frac{e_t \times L_t}{L + L_t}. \quad (16)$$

From Eq. (14), ϵ is inversely proportional to $\sqrt{m(1-2\eta)^2}$. Therefore, the condition $\epsilon_t < \epsilon_{t-1}$ is equivalent to

$$(L + L_t) \left(1 - 2 \times \frac{e_t \times L_t}{L + L_t} \right)^2 > (L + L_{t-1}) \left(1 - 2 \times \frac{e_{t-1} \times L_{t-1}}{L + L_{t-1}} \right)^2 \quad (17)$$

A sufficient condition for $\epsilon_t < \epsilon_{t-1}$ is

$$\begin{cases} L_t > L_{t-1}, \\ e_t \times L_t < e_{t-1} \times L_{t-1}, \end{cases} \quad (18)$$

which can be equivalently expressed as

$$0 < \frac{e_t}{e_{t-1}} < \frac{L_{t-1}}{L_t} < 1. \quad (19)$$

Hence, we complete the proof. \square

Dataset	Domain	Categories	Train	Test
ImageNet	Natural picture	1,000	1.28M	50,000
Caltech101	Object picture	100	4,128	2,465
OxfordPets	Pet picture	37	2,944	3,669
StanfordCars	Car picture	196	6,509	8,041
Flowers102	Flower picture	102	4,093	2,463
Food101	Food picture	101	50,500	30,300
FGVCAircraft	Aircraft picture	100	3,334	3,333
SUN397	Scene picture	397	15,880	19,850
DTD	Texture picture	47	2,820	1,692
EuroSAT	Satellite picture	10	13,500	8,100
UCF101	Video frame	101	7,639	3,783
CIFAR-10	Natural picture	10	50,000	10,000
CIFAR-100	Natural picture	100	50,000	10,000
ImageNet-100	Natural picture	100	130,000	5,000

Table 5: Details on the datasets used in our experiments.

A.2. Proof of Theorem 1

Proof. Let e_t denote the true relative error rate of pseudo-labels at iteration t , and let \hat{e}_t denote its estimated value computed on the labeled dataset at the same iteration. We begin by assuming that, during the course of training, the ratio of the true error rates between two consecutive iterations can be closely approximated by a power-law function of the corresponding ratio of the estimated error rates, given by:

$$\frac{e_t}{e_{t-1}} \approx \left(\frac{\hat{e}_t}{\hat{e}_{t-1}} \right)^{\alpha t} \quad (20)$$

where α is a scaling factor characterizing the rate of error reduction. Substituting this relationship into the condition in Eq. (19), we obtain

$$0 < \left(\frac{\hat{e}_t}{\hat{e}_{t-1}} \right)^{\alpha t} < \frac{L_{t-1}}{L_t} < 1 \quad (21)$$

Therefore, the maximum allowable number of pseudo-labeled samples at iteration t is given by

$$L_t^* = \left\lceil \left[\left(\frac{\hat{e}_{t-1}}{\hat{e}_t} \right)^{\alpha t} \times L_{t-1} - 1 \right] \right\rceil \quad (22)$$

In addition, the number of pseudo-labeled samples at iteration $t-1$ must satisfy

$$L_{t-1} < \left\lceil \left[\left(\frac{\hat{e}_{t-1}}{\hat{e}_t} \right)^{\alpha t} \times L_{t-1} - 1 \right] \right\rceil \quad (23)$$

which is equivalent to

$$L_{t-1} > \frac{\hat{e}_t^{\alpha t}}{\hat{e}_{t-1}^{\alpha t} - \hat{e}_t^{\alpha t}} \quad (24)$$

Consequently, we obtain both the upper bound on the number of pseudo-labeled samples at iteration t and the corresponding lower bound constraint on L_{t-1} . \square

Transformation	Description	Parameter	Value
<i>Weak Augmentations</i>			
RandomHorizontalFlip	Flips the image horizontally with a probability of p .	p	0.5
RandomCrop	Crops a random patch of the image after padding.	size padding	(224, 224) 28
<i>Strong Augmentations</i>			
ColorJitter	Randomly changes the brightness, contrast, saturation, and hue.	brightness	0.4
		contrast	0.4
		saturation	0.1
		hue	0.4
RandomGrayscale	Converts the image to grayscale with a probability of p .	p	0.2
GaussianBlur	Applies Gaussian blur to the image with a probability of p .	kernel_size	21
		p	0.5

Table 6: Details of Weak and Strong Data Augmentations.

B. Implementation Details

Dataset Details. We evaluate our method on 14 recognition datasets, comprising 11 commonly used benchmarks for evaluating vision-language models (VLMs) and 3 classical benchmarks for semi-supervised learning. These datasets include CIFAR-10 and CIFAR-100 (Krizhevsky, Hinton et al. 2009), ImageNet and ImageNet-100 (Deng et al. 2009), Caltech101 (Fei-Fei, Fergus, and Perona 2004), OxfordPets (Parkhi et al. 2012), StanfordCars (Krause et al. 2013), Food101 (Bossard, Guillaumin, and Van Gool 2014), Flowers102 (Nilsback and Zisserman 2008), FGVC Aircraft (Maji et al. 2023), SUN397 (Xiao et al. 2010), UCF101 (Soomro, Zamir, and Shah 2012), DTD (Cimpoi et al. 2014), and EuroSAT (Helber et al. 2019).

For ImageNet, Caltech101, OxfordPets, StanfordCars, Flowers102, FGVC Aircraft, SUN397, UCF101, DTD, and EuroSAT, we follow the dataset splits used in CoOp (Zhou et al. 2022a). For CIFAR-10, CIFAR-100, and ImageNet-100, we adopt the standard semi-supervised splits used in FixMatch (Sohn et al. 2020). Detailed statistics of these datasets are provided in Table 5. Specifically, for the open-world generalization experiment, we follow the standard base-to-novel setting (Zhou et al. 2022a), where base and novel classes are split evenly. We sample 16 shots per class as labeled data, and treat all remaining training samples as unlabeled. Due to computational constraints, for ImageNet we randomly sample 5% of the unlabeled set for training.

Training Details. As a plug-and-play method, Bi-CoG can be seamlessly integrated into any pretrain–finetune paradigm. In our experiments, we adopt CoOp (Zhou et al. 2022b), MaPLe (Khattak et al. 2023a), and PromptSRC (Khattak et al. 2023b) as the base methods, keeping all hyperparameters identical to those reported in their original papers. Unless otherwise specified, we set the number of models to $K = 3$ and the scaling factor to $\alpha = 1$. In the dynamic self-training stage, each model is first warmed

Dataset	CoOp		MaPLe		PromptSRC	
	ζ	κ	ζ	κ	ζ	κ
CIFAR-100	15	1	5	1	15	1
ImageNet	15	3	5	1	15	1
FGVCAircraft	15	3	5	1	20	1
SUN397	15	3	5	1	15	1
UCF101	15	3	5	1	15	1
CIFAR-10	15	3	5	1	15	3
DTD	15	3	5	1	15	1
EuroSAT	15	3	7	1	5	20
StanfordCars	15	3	7	1	5	20
ImageNet-100	15	5	5	1	15	3
Caltech101	20	5	5	1	20	5
OxfordPets	20	5	7	1	15	1
Flowers102	20	5	5	1	20	5
Food101	20	5	5	1	15	1

Table 7: Details of the training epoch.

up for ζ epochs using a small set of labeled data. Then, we apply our three-stage pseudo-label selection strategy to obtain pseudo-labels with high accuracy and low model bias, which are further used for self-training over κ additional epochs. The detailed parameters are provided in Table 7. During the intra-model consistency stage, we apply weak and strong augmentations to each sample, with the specific augmentation strategies summarized in Table 6. We conduct all experiments on a single NVIDIA A800 GPU.